Supplementary information

Bid-induced structural changes in BAK promote apoptosis

Tudor Moldoveanu[1], Christy R. Grace[2], Fabien Llambi[1], Amanda Nourse[3], Patrick Fitzgerald[1], Kalle Gehring[4], Richard W. Kriwacki[2,5] and Douglas R. Green[1]

Affiliations:

[1]Department of Immunology, St. Jude Children's Research Hospital, Memphis, Tennessee, USA.

[2]Department of Structural Biology, St. Jude Children's Research Hospital, Memphis, Tennessee, USA.

[3]Hartwell Center for Bioinformatics and Biotechnology, St. Jude Children's Research Hospital, Memphis, Tennessee, USA.

[4]Department of Biochemistry, McGill University, Montreal, Canada.

[5]Department of Microbiology, Immunology and Biochemistry, University of Tennessee Health Sciences Center, Memphis, Tennessee, USA.

Inventory of items in the Supplementary information

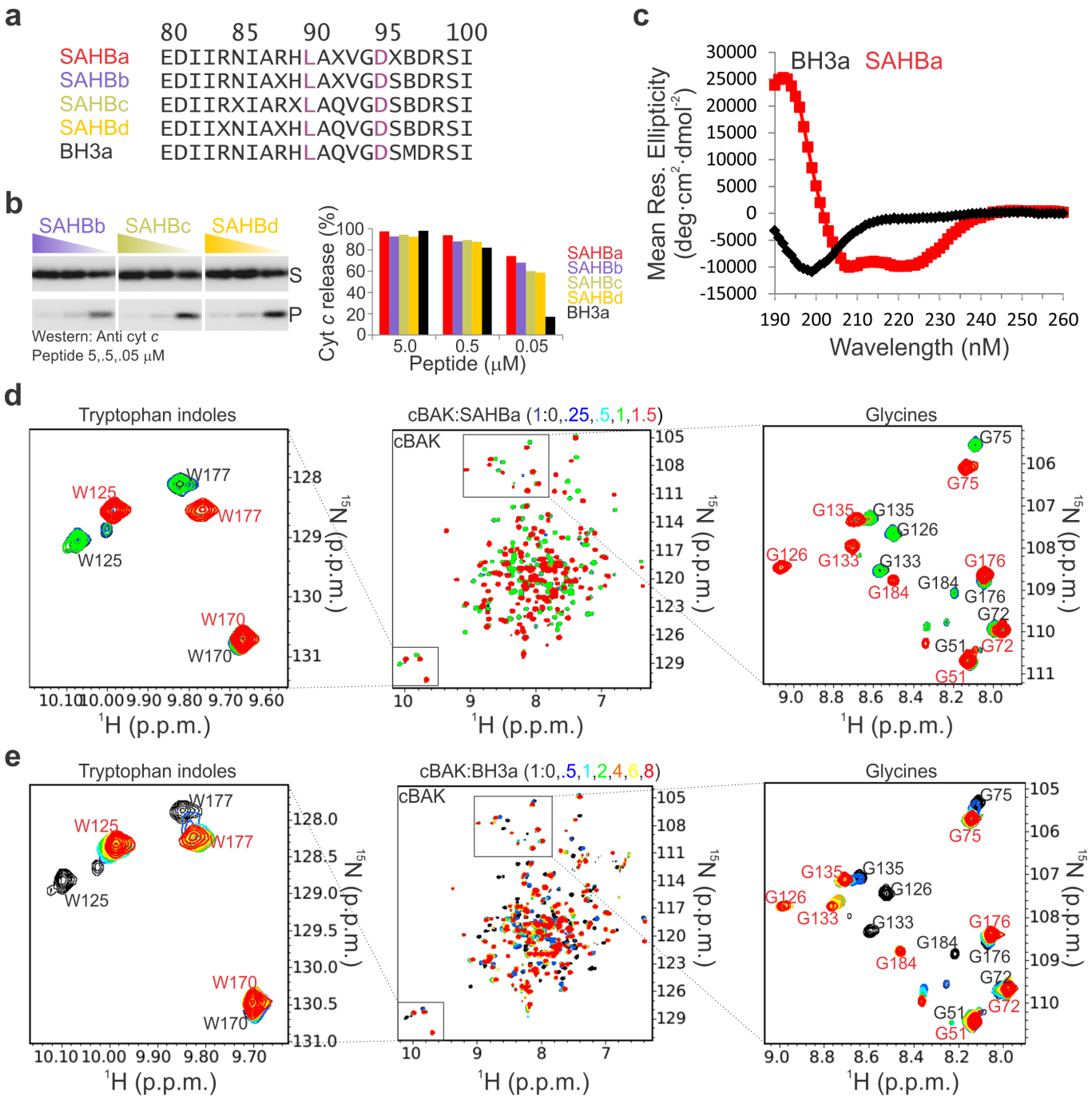

Supplementary Figure 1. Helical stapled BID BH3 peptides induce potent direct BAK activation and MOMP by binding the BC groove

(a) Alignment of BID BH3 peptides identifying the non-natural amino acids including the stabilizing bridge pentylalanine positions (X) and norleucine (B). Conserved BH3 residues are colored.

(b) MOMP assays tested cyt *c* release from purified B6 mouse liver mitochondria after 45 min incubations with the peptides at 5, 0.5 and 0.05 μM. Cyt *c* in the supernatant (S) and pellet (P) was

assessed by Western blotting. Bands from these and images in Fig. 1b were integrated by densitometry to calculate cyt *c* release, which is represented as histograms.

(c) CD analysis of 25 μM BID peptides in 10 mM phosphate buffer (pH 7.0) were performed at 25°C. The stapled SAHBa displayed a helical peptide conformation with minima at 208 and 222 nm, while the unstapled BH3a showed a typical intrinsically disordered profile.

(d-e) [^{15}N/^{1}H] TROSY spectra of 150 μM ^{15}N-cBAK with indicated molar equivalents of SAHBa (d) and BH3a (e). Regions corresponding to the tryptophan indoles and glycines were expanded to illustrate the high degree of similarity between peptide-induced spectral changes. Due to its weaker binding affinity for cBAK, more BH3a was required to induce spectral changes seen with 1:1 molar equivalents of SAHBa–cBAK.

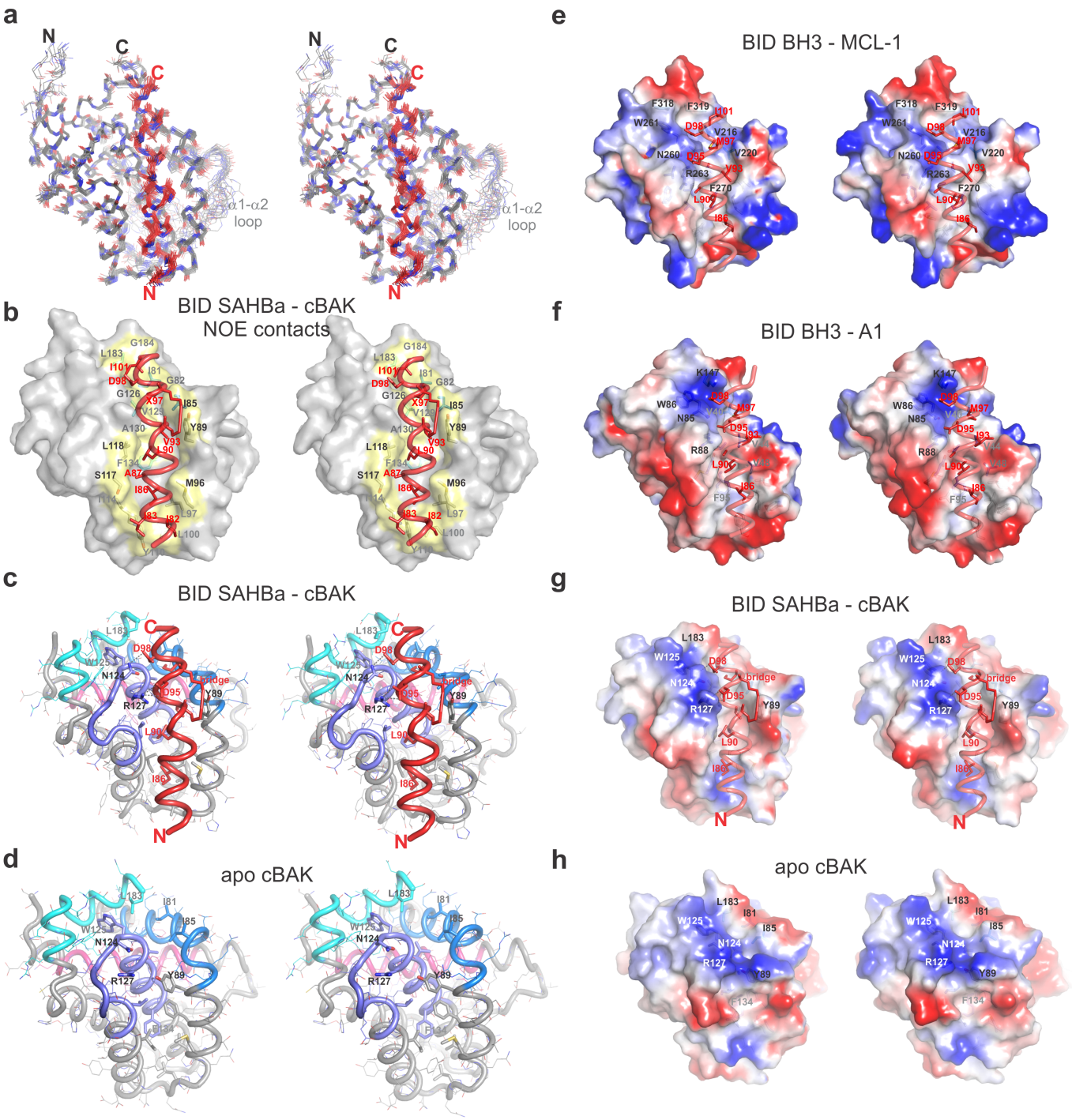

Supplementary Figure 2. High-resolution details of BAK direct activation by BID reveal unique rearrangement of the BH1-BH3 hydrophobic core

This is the first high-resolution structure of BAK in complex with an activator BH3-only peptide, which facilitated the unambiguous identification of the BC groove as the trigger site of BAK. We subjectively describe the interactions by SAHBa at the trigger site of BAK. The "bottom" of the BC

groove (Fig. 2, Supplementary Fig. 2 “front view”) is seemingly looser as it widens and the pockets are poorly defined with the SAHBa N-terminal Ile82 and Ile83 reaching towards His99 and Lys113, respectively, while resting on top of a hydrophobic bed defined by Leu100 and Tyr110. As the SAHBa folds its second turn, the first deep cavity lined by Met96, Leu97, Leu100, and Ile114 of BAK is evident accommodating Ile86 side chain at its lower periphery. The third turn of SAHBa is dominated by Leu90, which defines a shallow pocket lined tightly by Phe93, Met96, Ile114, and Leu118 of BAK. This is followed along the groove by Val93 of the fourth SAHBa turn, which touches deep within yet another cavity lined by Asn86, Ile85, Tyr89, and Phe93 side chains from the BH3 of BAK on one side and Ala130 on the other side. The fifth SAHBa turn presents an extended norleucine (Nle97) side chain, as an oxidation resistant Met97 analog, which fits a pocket lined by Gly82, Asn86, and Ile85 of the BH3 of BAK on one side and Gly126, Val129, and Ala130 of the BH1 on the other side. Together, Ile86, Leu90, Val93, and Nor97 of SAHBa positioned central within the BC groove, appear to define wedge-like sites that force the C-terminal BH3 sequence of BAK (residues Ile85 to Tyr89) from making the hydrophobic contacts predicted to occlude the BC groove in the free BAK structure (Fig. 2, Supplementary Movies 1, 2). This outward BH3 movement of BAK creates the deepest empty cavity in the complex bounded by Val93 and Nor97 of SAHBa. The position occupied by the sixth SAHBa turn helps project Ile101 side chain towards a shallow hydrophobic surface defined by Ile83 of the BH3, Trp125 of the BH1 and Leu183 and Gly184 of the BH2 of BAK.

(a) Stereo view of the superimposition of 20 lowest-energy NMR structures (Table 1).

(b) Stereo view showing the intermolecular NOE contact used in the structure calculation of SAHBa–cBAK complex.

(c, d, g, h) Stereo view of region undergoing conformational changes in SAHBa–cBAK (c, g) and apo cBAK (d, h; 2IMT).

(e-f) Stere oview of BID BH3 interactions at the BC groove of MCL-1 (e, 2KBW) and A1 (f, 2VOI).

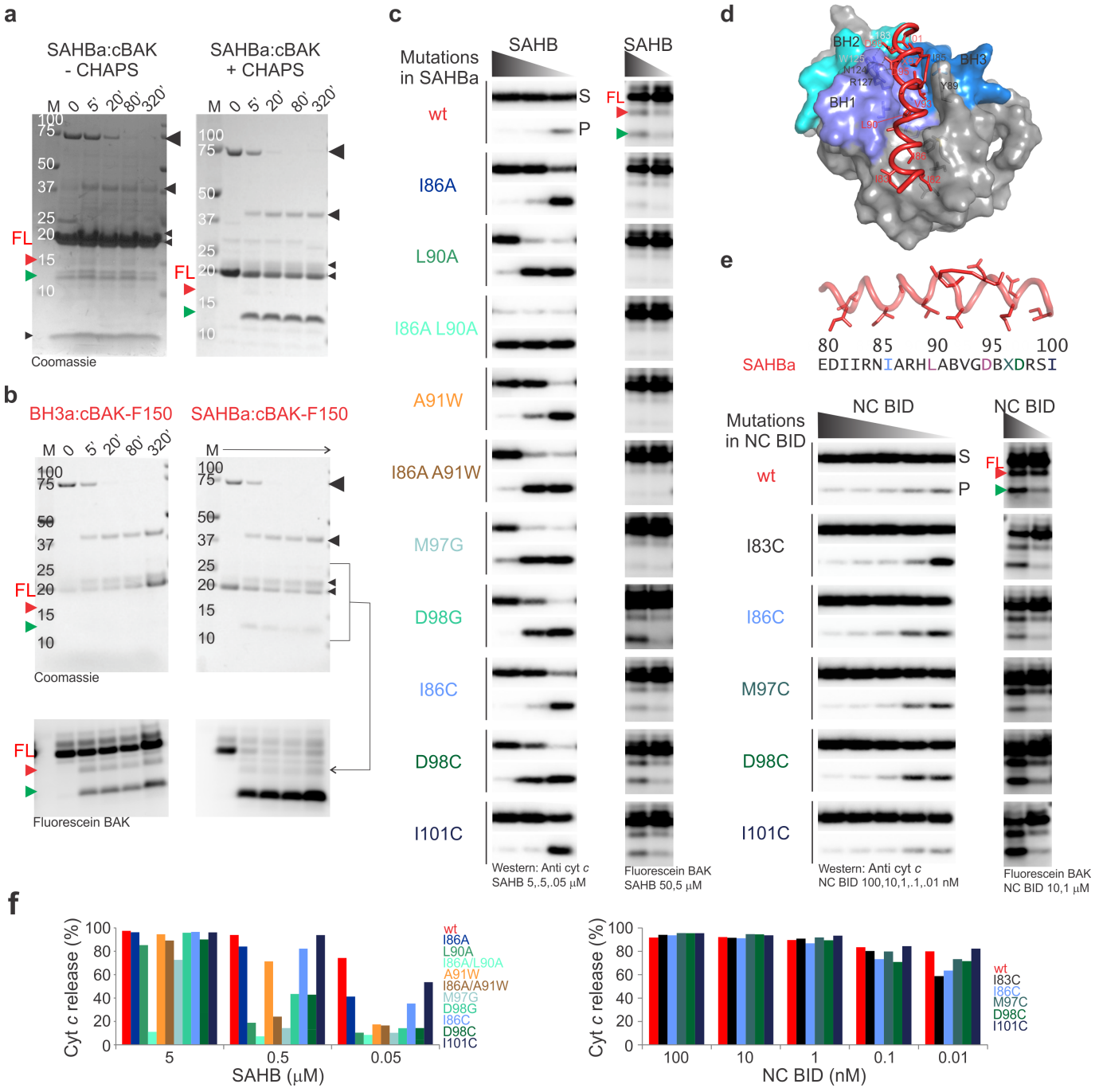

Supplementary Figure 3. Correlation of MOMP with conformational changes induced by BID in BAK

(a) Protease sensitivity assays in the presence (right) or absence of 1% CHAPS (left) were performed in 50 mM HEPES pH 7.5, 10 mM dithiothreitol (DTT), 1 μM m-calpain, and 0.5 mM $CaCl_2$.

The 1.5:1 SAHBa–^{15}N-cBAK complex (~150 μM) digested in the absence of CHAPS (left) was taken from the NMR titration analysis presented in Supplementary Fig. 1D. Concentrations of 50 μM cBAK and 50 μM peptides were used with CHAPS (right). Gel images identify calpain and its autoproteolytic breakdown products (right hand black arrowheads) and full-length cBAK (FL) and its fragments (red and green arrowheads). Stapled BID peptides, but not unstapled (not shown), were resistant to calpain proteolysis (left hand black arrowhead).

(b) Protease sensitivity assays probed BAK conformation in 50 mM HEPES pH 7.5, 10 mM dithiothreitol (DTT), 1 μM m-calpain, 0.5 mM $CaCl_2$, 1% CHAPS, and 25 μM cBAK derivatized at Cys166 with the thiol-reactive F150 fluorescein tag (cBAK-F150) and 25 μM peptides at 24°C. cBAK-F150 and its calpain-generated fragments allowed enhanced detection during SDS-PAGE analysis by fluorescein imaging. Upper panels represent m-calpain autoproteolysis fragments; m-Calpain autolysis dissipated its activity by 80 min, producing 3 stable fragments (black arrowhead). cBAK (FL) proteolysis by calpain produced two faintly stained fragments (red and green arrows). Lower panels show the corresponding fluorescein images identifying cBAK-F150 fragments.

(c, e and f) MOMP (left) and protease sensitivity assays (right) were performed as in Fig. 3b, c with the indicated direct activators. The protease sensitivity assay for D98G shown is one of two independent experiments distinct from that of the other conditions, and showed slightly different kinetics in the SAHBa control (not shown). Bands from images in (c) and (e) were integrated by densitometry and cyt *c* release was calculated and is represented in (f).

(d) Surface-cartoon representation of the SAHBa–cBAK BC groove view.

The MOMP and protease sensitivity assays were performed at the same time for all BID ligands. Representative profiles were extracted from larger images.

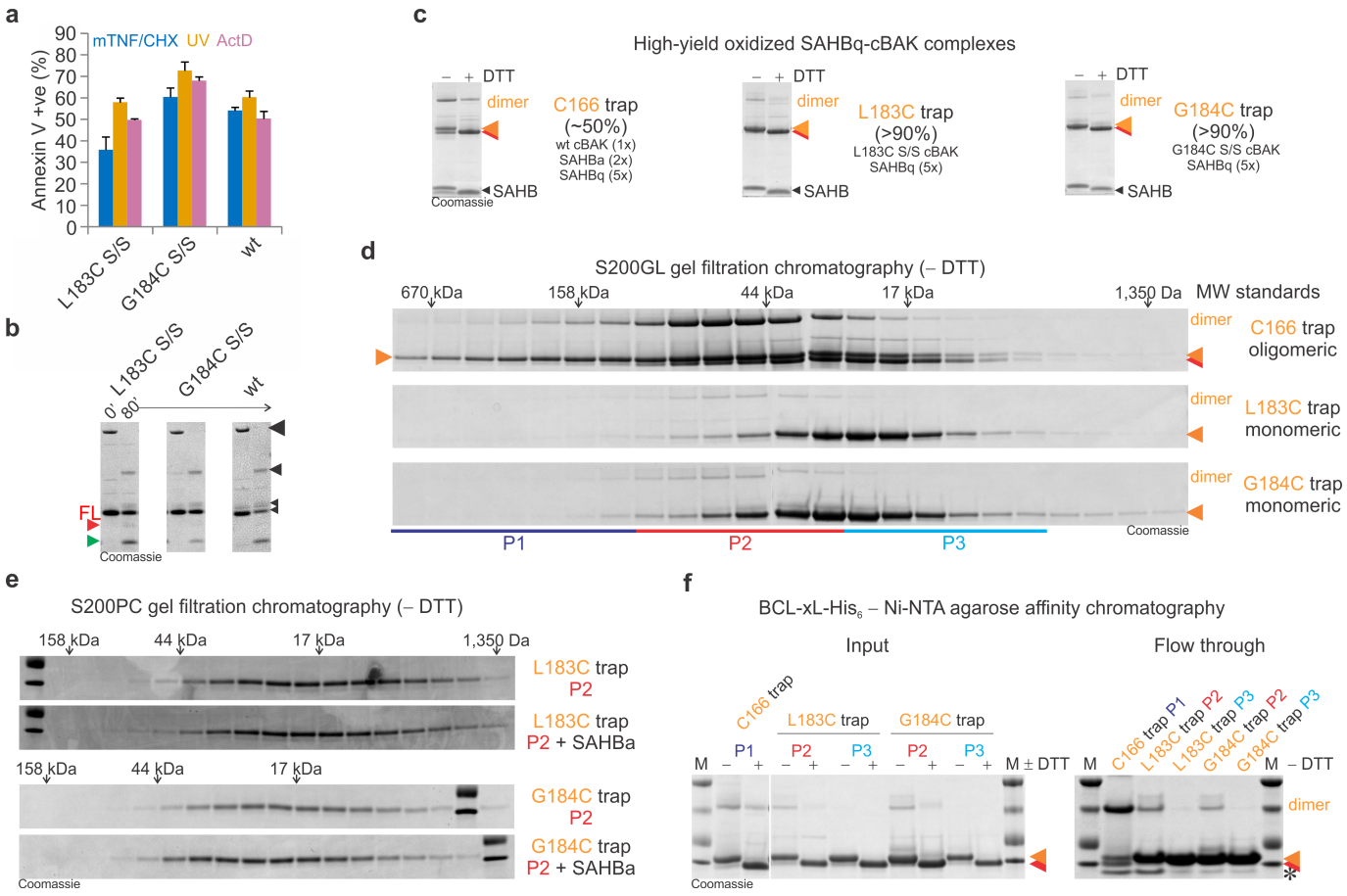

Supplementary Figure 4. Bound activators at the BC groove of BAK must be displaced for activation

We introduced single cysteines at Leu183 and Gly184 (near BID Ile101) both of which retain apoptotic activity comparable to wt BAK when reconstituted in DKO MEFs.

(a) Cell death of wt and BAK mutants stably reconstituted in DKO MEFs was induced with 1 ng ml^{-1} mouse TNF and 0.5 μg ml^{-1} CHX, 5 mJ UV, or 0.5 μM ActD. After 24 h, the cells were prepared for FACS analysis to monitor the extent of apoptosis as measured by annexin V positivity. Cys14 and Cys166 were replaced by Ser (S/S). Data are represented as mean ± SD.

(b) Protease sensitivity assays of purified 20 μM wt or cBAK mutant, 50 μM SAHBa and 1 % CHAPS were performed as in Supplementary Fig. 3A. Full-length cBAK (FL).

(c) Oxidized SAHBq–cBAK traps were produced with high efficiency by Cu/Phe oxidation of the corresponding mixtures.

(d) Gel filtration chromatography profiles of the oxidized traps in (c) by SDS-PAGE. Elution peaks P1, P2, and P3 were pooled for further analysis.

(e) Gel filtration chromatography profiles of pooled P2 elution peaks of L183C and G184C trap (25 μM) in (d) ± SAHBa (100 μM).

(f) Input and flow through SDS-PAGE profiles of L183C and G184C traps in (c) from a BCL-xL-His_6 – Ni^{2+}-NTA agarose affinity column. BCL-xL-His_6 in the flow through is marked by *.

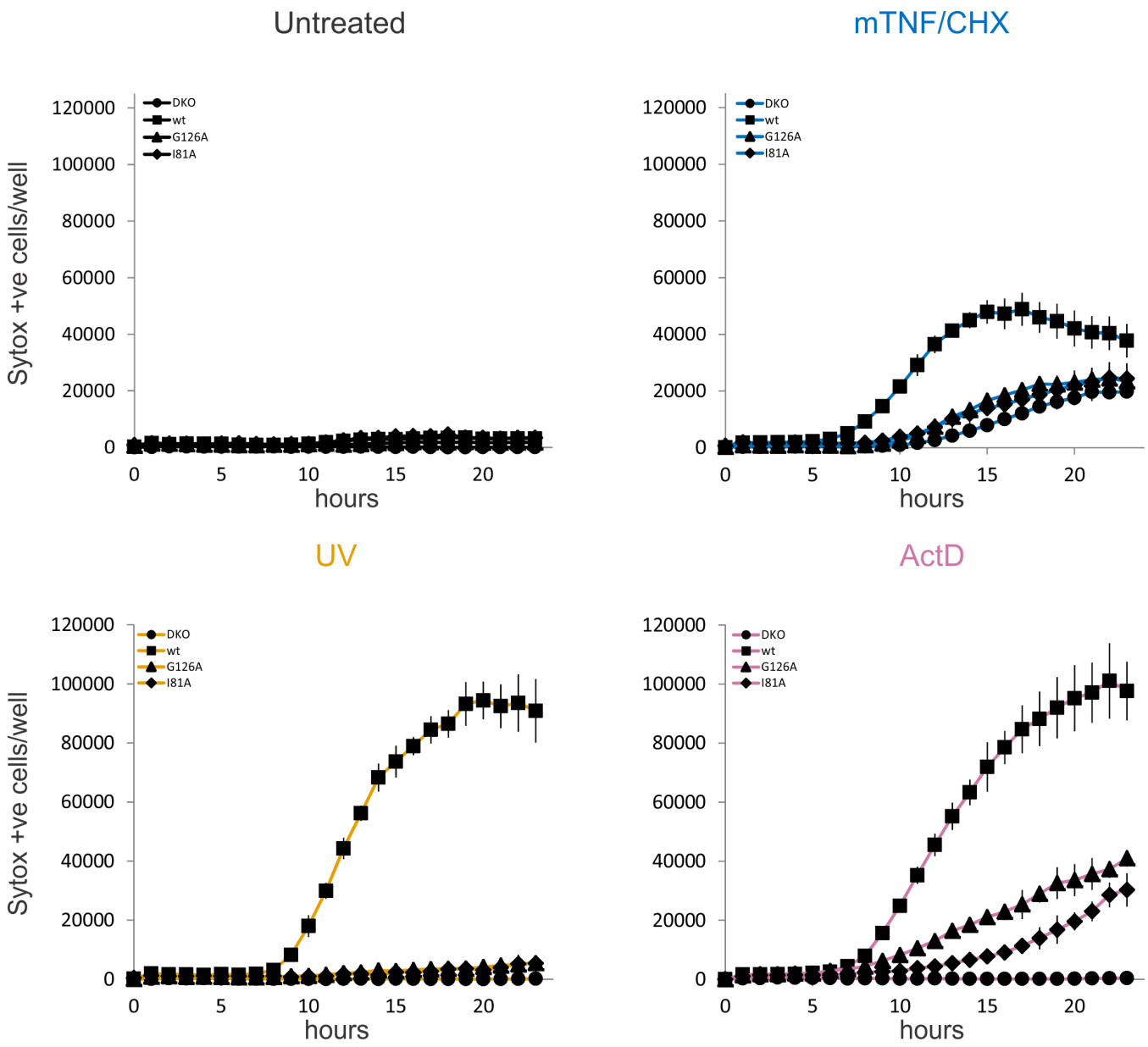

Supplementary Figure 5. Death by diverse apoptotic stimuli support a unifying direct BAK activation mechanism

Cell death of wt and BAK mutants stably reconstituted in DKO MEFs induced with 1 ng ml^{-1} mouse TNF and 0.5 mg ml^{-1} CHX, 5 mJ UV, or 0.5 μM ActD was monitored by hourly IncuCyte imaging in the presence of 10 nM Sytox green. Sytox green-positive dead cells are plotted for the first 23 h. The 24 h time point was used to measure apoptosis in Fig. 5c.

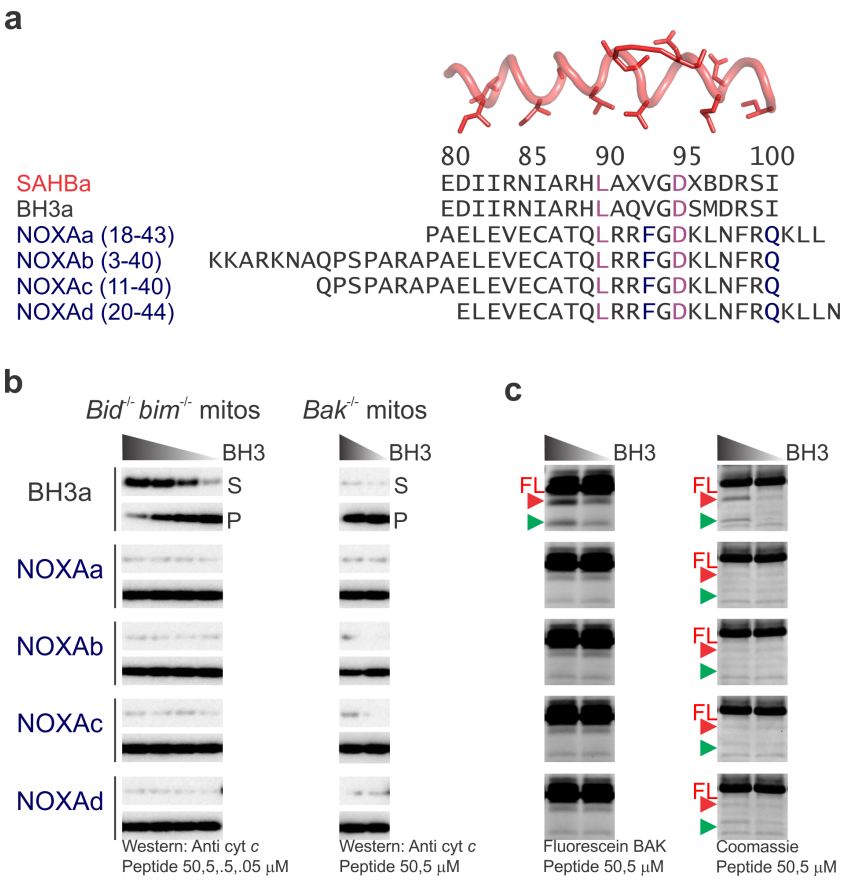

Supplementary Figure 6. NOXA is not a direct activator of BAK

(a) NOXA BH3 peptide alignment. NOXAa was previously shown to be inactive in inducing MOMP in digitonin-permeabilized *bid*$^{-/-}$ *bim*$^{-/-}$ MEFs[1].

(b) MOMP assays tested cyt *c* release from purified *bid*$^{-/-}$ *bim*$^{-/-}$ or *bak*$^{-/-}$ mouse liver mitochondria after 1 h incubations. Cyt *c* in the supernatant (S) and pellet (P) was assessed by Western blotting. A NOXA peptide corresponding to residues 20-54 of human NOXA induced MOMP in purified mitochondria from *bak*$^{-/-}$ livers and was therefore excluded from our analysis but may suggest that the previously observed activity of an E. coli-expressed NOXA may be attributed to its non-specific activity at non-physiologically high concentrations[2].

(c) Protease sensitivity assays with the respective peptides were performed as in Supplementary Fig. 3b.

The MOMP and protease sensitivity assays were performed at the same time for all BH3–BAK complexes. Representative profiles were extracted from larger images.

Supplementary Table 1. Summary of structure-function parameters for the BAK and BID proteins and peptide ligands used in this study.

BID BH3/SAHB peptides	80 85 90 95 100	NMR[a]	Affinity for BAK K_D (μM)[b]	Protease sensitivity[c]	MOMP threshold B6 liver mitos (μM)[d]
hBID_BH3a – wt 80-101	EDIIRNIARHLAQVGDSMDRSI	✓	10.12 ± .0019	✓	5/.5/.05
hBID_SAHBa – wt 80-101	EDIIRNIARHLAXVGDXBDRSI	✓	.89 ± .0023	✓	5/.5/.05
hBID_SAHBb – bridge 88 – 92	EDIIRNIAXHLAXVGDSBDRSI	✓	1.27 ± .0028	✓	5/.5/.05
hBID_SAHBc – bridge 85 – 89	EDIIRXIARXLAQVGDSBDRSI	×	.84 ± .0047	✓	5/.5/.05
hBID_SAHBd – bridge 84 – 88	EDIIXNIAXHLAQVGDSBDRSI	×	1.02 ± .0025	✓	5/.5/.05
hBID_SAHBe – wt 80-104	EDIIRNIARHLAXVGDXBDRSIPPG	✓	.85 ± .0024	✓	5/.5/.05
hBID_SAHBf – ΔN-turn1	RNIARHLAXVGDXBDRSI	×	4.42 ± .0035	✓	5/.5/.05
hBID_SAHBg – ΔN-turn1-2	RHLAXVGDXBDRSI	×	9.43 ± .0041	×	5/.5/.05
hBID_SAHBh – I86A	EDIIRNAARHLAXVGDXBDRSI	✓	1.04 ± .0026	✓	5/.5/.05
hBID_SAHBi – L90A	EDIIRNIARHAAXVGDXBDRSI	×	ND	×	5/.5/.05
hBID_SAHBj – I86A/L90A	EDIIRNAARHAAXVGDXBDRSI	×	ND	×	5/.5/.05
hBID_SAHBk – A91W	EDIIRNIARHLWXVGDXBDRSI	×	ND	×	5/.5/.05
hBID_SAHBl – I86A/A91W	EDIIRNAARHLWXVGDXBDRSI	×	ND	×	5/.5/.05
hBID_SAHBm – I86C	EDIIRNCARHLAXVGDXBDRSI	ND	ND	✓	5/.5/.05
hBID_SAHBn – M97G	EDIIRNIARHLAXVGDXGDRSI	ND	ND	✓	5/.5/.05
hBID_SAHBo – D98G	EDIIRNIARHLAXVGDXBGRSI	ND	ND	ND	5/.5/.05
hBID_SAHBp – D98C	EDIIRNIARHLAXVGDXBCRSI	ND	4.13 ± .0028	✓	5/.5/.05
hBID_SAHBq – I101C	EDIIRNIARHLAXVGDXBDRSC	✓	1.06 ± .0024	✓	5/.5/.05
N/C BID Proteins	80 85 90 95 100				(nM)
N/C BIDa – wt	EDIIRNIARHLAQVGDSMDRSI	×		✓	100/10/1/.1/.01
N/C BIDb – I83C	EDICRNIARHLAQVGDSMDRSI	ND		✓	100/10/1/.1/.01
N/C BIDc – I86A	EDIIRNAARHLAQVGDSMDRSI	ND		✓	100/10/1/.1/.01
N/C BIDd – I86C	EDIIRNCARHLAQVGDSMDRSI	ND		✓	100/10/1/.1/.01
N/C BIDe – L90A	EDIIRNIARHAAQVGDSMDRSI	ND		✓	100/10/1/.1/.01
N/C BIDf – I86A/L90A	EDIIRNAARHAAQVGDSMDRSI	ND		✓	100/10/1/.1/.01
N/C BIDg – A91W	EDIIRNIARHLWQVGDSMDRSI	ND		✓	100/10/1/.1/.01
N/C BIDh – I86A/A91W	EDIIRNAARHLWQVGDSMDRSI	ND		✓	100/10/1/.1/.01
N/C BIDi – M97C	EDIIRNIARHLAQVGDSCDRSI	ND		✓	100/10/1/.1/.01
N/C BIDj – M97G	EDIIRNIARHLAQVGDSGDRSI	ND		✓	100/10/1/.1/.01
N/C BIDk – D98C	EDIIRNIARHLAQVGDSMCRSI	ND		✓	100/10/1/.1/.01
N/C BIDl – D98G	EDIIRNIARHLAQVGDSMGRSI	ND		✓	100/10/1/.1/.01
N/C BIDm – I101C	EDIIRNIARHLAQVGDSMDRSC	ND		✓	100/10/1/.1/.01
NOXA BH3/SAHB peptides	5 10 15 20 25 30 35 40				(nM)
NOXAa (18-43)	PAELEVECATQLRRFGDKLNFRQKLL	×	ND	×	50/5/.5/.05
NOXAb (4-40)	KKARKNAQPSPARAPAELEVECATQLRRFGDKLNFRQ	ND	ND	×	50/5/.5/.05
NOXAc (11-40)	QPSPARAPAELEVECATQLRRFGDKLNFRQ	ND	ND	×	50/5/.5/.05
NOXAd (20-44)	ELEVECATQLRRFGDKLNFRQKLLN	ND	ND	×	50/5/.5/.05
NOXA SAHB	QPSPARAPAELEVECATQLRXFGDXLNFRQ	ND	ND	×	50/5/.5/.05
NOXA/BID a	AELEVECATQLRRVGDKLNFRI	ND	ND	×	50/5/.5/.05
NOXA/BID b	AELEVECATQLRRFGDKLNFRI	ND	ND	×	50/5/.5/.05
NOXA/BID c	AELEVECATQLRRVGDKLNFRQ	ND	ND	×	50/5/.5/.05
NOXA/BID d	AELIVECATQLRRFGDKLNFRQ	ND	ND	×	50/5/.5/.05
NOXA/BID e	AEIIVECATQLRRFGDKLNFRQ	ND	ND	×	50/5/.5/.05
NOXA/BID f	AEIIVECATQLRRVGDKLNFRI	ND	ND	×	50/5/.5/.05
BAD BH3/SAHB peptides	105 110 115 120 125				(nM)
BADa (103-127)	NLWAAQRYGRELRRMSDKFVDSFKK	×	ND	×	50/5/.5/.05
BAD SAHB	LWAAQRYGRELRXMSDXFVDSF	ND	ND	×	50/5/.5/.05
BAD/BID a	LWAAQRIGRELRRMGDEMVDSI	ND	ND	✓	50/5/.5/.05

BAK proteins	Mutation region/effect		Affinity for SAHBa K_D (μM)[e]		MOMP threshold BAK in DKO MEFs N/C BID (nM)
wt		✓	.94 ± .0030	✓	100/10/1/.1/.01
G126A	BH1/blocked direct activation	✓	.98 ± .0026	×	100/10/1/.1/.01
I81A	BH3/blocked oligomerization	✓	.97 ± .0028	✓	100/10/1/.1/.01

[a] ^{15}N-^{1}N TROSY NMR titrations shown in Fig. 2 and Supplementary Fig. 2 were performed for the indicated peptides using 5× and 20× molar excess over wt or BAK mutants. BID peptides that showed binding to BAK similar to that of SAHBa and the BAK mutants that bound to SAHBa are ✓ marked. We found that some peptides did not conform to the slow exchange observed for the SAHBa–cBAK interaction, but rather displayed an intermediate exchange as we observed in ref. 18. We therefore scored this as not binding by NMR (×) because we did not observe the signature

bound conformation induced by potent BID peptides that display slow exchange kinetics in the complex with BAK. ND not determined.

[b] Affinity of BH3 peptides was estimated from sedimentation equilibrium AUC experiments (Supplementary Table 2).

[c] Protease sensitivity assays were performed at least twice with all BID ligands as illustrated in Supplementary Fig. 3C.

[d] MOMP assays were performed at least twice with all BH3 ligands as illustrated in Figs. 1, 3, and 6. Red, violet, and black colors represent the extent of cyt *c* release, respectively, high, moderate to low, and undetectable. DMSO, BH3s (50 μM), or SAHBs (5 μM) alone did not permeabilize *bak*$^{-/-}$ mitochondria.

[e] Affinity of SAHBa for wt and BAK mutants was estimated from sedimentation equilibrium AUC experiments (Supplementary Table 2).

X and B are the pentenylalanine and the methionine analogue norleucine, respectively.

Supplementary Table 2. Summary of results of the sedimentation equilibrium experiments of BAK interaction with BID peptides in 20 mM HEPES, 100 mM NaCl, and 0.5 mM DTT at 20°C. Models used: single species as well as the single-site hetero-association model (A+B↔AB with the peptide species A and cBAK species B).

Sample	μM[a]	K_{AB} (μM)[b]	R.m.s.d.[c]	MW (kDa)[d]	R.m.s.d.[e]
wt cBAK + BH3a	12.8&4.0	10.12	0.0019	21.675 (21.690)	0.0019
wt cBAK + SAHBa	13.6&4.0	0.89	0.0023	22.305 (21.725)	0.0021
wt cBAK + SAHBb	25.0	1.27	0.0028	21.7	0.0028
wt cBAK + SAHBc	24.0	0.84	0.0047	20.0	0.0049
wt cBAK + SAHBd	25.0	1.02	0.0025	21.7	0.0025
wt cBAK + SAHBe	13.9&3.6	0.85	0.0024	22.013 (21.976)	0.0024
wt cBAK + SAHBf	18.0	4.42	0.0035	19.5	0.0035
wt cBAK + SAHBg	25.0	9.43	0.0041	18.9	0.0041
wt cBAK + SAHBh	13.0&3.9	1.04	0.0026	21.211 (21.683)	0.0026
wt cBAK + SAHBp	25.0	4.13	0.0028	20.7	0.0029
wt cBAK + SAHBq	14.1&4.1	1.06	0.0024	22.168 (21.715)	0.0026
wt cBAK + SAHBa	26.0	0.94	0.0030	22.7	0.0029
G126A cBAK + SAHBa	24.0	0.98	0.0026	21.9	0.0027
I81A cBAK + SAHBa	22.0	0.97	0.0028	21.6	0.0028

[a] Total loading concentrations in μM of sample (left) and at ~ 3-fold lower concentration (right).

[b] K_{AB} is the dissociation constant for the reversible single-site hetero-association of peptide (species A) and cBAK (species B).

[c] Root mean square deviation in absorbance units of the fit to the reversible single-site hetero-association model.

[d] Fitted molar mass of single species model with theoretical molar mass of the BAK–BID peptide complex in parentheses.

[e] Root mean square deviation of the fit; units in absorbance.

Supplementary Movie 1. "Front view" of BID-induced conformational change in BAK

Movie captures the conformational changes of apo to SAHBa–bound cBAK described in Fig. 2 and Supplementary Fig. 2. LSQMAN[3] was used to generate the frames and Pymol to render them.

Supplementary Movie 2. "Side view" of BID-induced conformational change in BAK

Movie captures the conformational changes of apo to SAHBa–bound cBAK from a side view compared to that of Supplementary Movie 1.

Supplementary Note

Direct activation assays – calpain protease sensitivity in CHAPS

We recently presented a protease sensitivity assay to determine the activation state of BAK during MOMP reactions with purified mitochondria containing native BAK, in digitonin permeabilized cells undergoing apoptosis and in NP40 detergent with purified bacterial expressed proteins[4]. We adapted this assay to a cell- and mitochondria-free system by using a CHAPS-based buffer, which, unlike the NP40-based buffer[5], does not have the ability to activate BAK but can support its activation in the presence of a direct activator[2]. The protease sensitivity assay was performed for up to two hours in 50 mM HEPES pH 7.5, ±1% CHAPS, ±10 mM DTT (depending on the desired oxidation status of the reaction) and containing up to 1 μM m-calpain protease that was activated with 0.5 mM $CaCl_2$. Various BAK proteins, including wild-type (wt), mutants, and cBAK-F150, as well as SAHBq–cBAK disulfide-trapped complexes, were tested at concentrations up to 50 μM. BID direct activator ligands were tested at ranges up to 20 μM for purified NC BID and 100 μM for BID BH3 and BID SAHB. At specific times, the proteolysis was stopped with sodium dodecyl sulfate (SDS) sample buffer, and SDS-PAGE analysis was later performed. All gels were stained with Coomassie brilliant blue r-250. cBAK-F150 gels were imaged prior to staining using a Carestream 4000MM Pro imaging system.

MOMP, BMH cross-linking and protease sensitivity assays

Our standard MOMP assay follows previously detailed protocols[4] based on differential centrifugation in a minimal mitochondrial isolation buffer (MIB) composed of 200 mM mannitol, 68 mM sucrose, 10 mM HEPES (pH 7.4), 10 mM KCl, and 1 mM EDTA and supplemented with Complete Protease Inhibitor (Roche). The MOMP reactions proceeded for 45 min to 1 h at 37°C in a total volume of 50 μL. In addition to MIB, they also contained one of the following BID direct activator ligands at the indicated concentrations: purified NC BID at 10 pM–250 nM; BID SAHB peptides at 50 nM–5 μM; NOXA and BAD SAHB peptides at 50 nM–50 μM; or BID, NOXA, BAD, NOXA/BID and BAD/BID BH3 peptides at 50 nM–50 μM. For MOMP reaction with cBAK and SAHBq–cBAK traps, the protein concentration was up to 5 μM. Mitochondria were isolated from livers of B6, *bak*$^{-/-}$, and *bid*$^{-/-}$ *bim*$^{-/-}$ mice. To exclude BAK-independent peptide-mediated MOMP, all peptides were tested alone in *bak*$^{-/-}$ reactions to establish a suitable range of concentrations for BAK direct activation. The reactions were subjected to centrifugation to separate the pellets and supernatants, and both fractions were quenched by the addition of SDS sample buffer. To monitor the extent of permeabilization, both fractions were immunoblotted with anti cyt *c* monoclonal antibody (BD Biosciences).

Thiol-directed cross-linking of wt and BAK mutants reconstituted in DKO MEFs was performed on the MOMP reaction mitochondrial pellet by an additional 30 min incubation at 24°C with 0.5 μM bismaleimidohexane (BMH, Pierce). Similarly, protease sensitivity assays were performed on MOMP reactions by an additional 45 min incubation with 20 nM m-calpain and 0.5 mM $CaCl_2$ in MIB without EGTA. Cross-linking and proteolysis were monitored by Western blotting with anti-BAK Ab-1 and G23 antibodies.

Oxidation of "trapped" SAHB–BAK complexes

Oxidation reactions of BID–BAK complexes at engineered free cysteines in BID and BAK were performed using the copper/phenanthroline (Cu/Phe) oxidizing agent from a 4:1 water:ethanol-based 100× stock at 30 mM $CuSO_4$ and 100 mM 1,10-phenanthroline (Sigma). The oxidation reactions performed at 24°C were buffered to 50 mM HEPES, pH 7.5, and, in addition to the 1× Cu/Phe oxidation reagent, contained up to 100 μM cBAK mutant or SAHBq–cBAK mutant combinations as follows: i) for all low-efficiency reactions, 20 μM wt or cBAK mutants and 50 μM SAHBq; ii) for all high-efficiency reactions, 100 μM wt or cBAK mutants and 500 μM SAHBq, except for the Cys166 trap reaction, which also contained 200 μM SAHBa mixed in first to block SAHBq binding to the BC groove. The oxidation reaction was stopped by the addition of ethylenediaminetetraacetic acid (EDTA) to a final concentration of 20 mM. The low-efficiency reactions were next washed 4 times in a 5 mL concentrator with a 10 kDa molecular weight cutoff in 20 mM HEPES, pH 7.0, to remove excess oxidizing reagents and unreacted peptide. The high-efficiency reactions were subjected to gel filtration chromatography on a S200GL column (GE Healthcare) and affinity chromatography on a BCL-xL-His_6–Ni^{2+}-NTA agarose column. SDS PAGE analysis was then performed in non-reducing and reducing conditions to assess the extent of disulfide bridging. The "trapped" oxidized SAHBq–cBAK complexes were tested in protease sensitivity and MOMP assays.

Cell death assays

Bak$^{-/-}$ *bax*$^{-/-}$ MEFs stably reconstituted with wt and BAK mutants were subjected to cell death assays repeated multiple times in duplicate using 24-well plates (BD Falcon) at 40-80% confluency. The apoptotic stimuli tested were mouse tumor necrosis factor (mTNF) up to 5 ng ml^{-1} in the presence of cycloheximide (0.5 mg ml^{-1}), Actinomycin D (ActD) up to 1 μM, or ultraviolet radiation (UV) up to 20 mJ. The cell death reactions were up to 24 h long with hourly monitoring by fluorescence imaging in an IncuCyte green fluorescence imaging system in the presence of 10 nM

Sytox green (Invitrogen), a nuclear staining dye used to monitor the extent of plasma membrane permeabilization. At 12 h and 24 h, the cells were prepared for FACS analysis to monitor the extent of apoptosis. Cells were trypsinized, washed once with PBS and stained with annexin V–APC (BD Biosciences) to prevent any interference with the GFP and Sytox. The FACS data were immediately collected on a Scan II flow cytometer (BD Biosciences) and later analyzed using FlowJo (www.FlowJo.com).

References

1. Du, H. et al. BH3 domains other than Bim and Bid can directly activate Bax/Bak. *J. Biol. Chem.* **286**, 491-501 (2011).
2. Dai, H. et al. Transient binding of an activator BH3 domain to the Bak BH3-binding groove initiates Bak oligomerization. *J. Cell Biol.* **194**, 39-48 (2011).
3. Kleywegt, G.J. Use of non-crystallographic symmetry in protein structure refinement. *Acta Crystallogr. D Biol. Crystallogr.* **52**, 842-57 (1996).
4. Llambi, F. et al. A unified model of mammalian BCL-2 protein family interactions at the mitochondria. *Mol. Cell* **44**, 517-31 (2011).
5. Liu, Q. & Gehring, K. Heterodimerization of BAK and MCL-1 activated by detergent micelles. *J. Biol. Chem.* **285**, 41202-10 (2010).